NANO-MICRO LETTERS ARTICLE
www.nmletters.org

Magnetic Fe_3O_4-Reduced Graphene Oxide Nanocomposites-Based Electrochemical Biosensing

Lili Yu, Hui Wu, Beina Wu, Ziyi Wang, Hongmei Cao, Congying Fu, Nengqin Jia*

(Received 29 January 2014; accepted 11 March 2014; published online July 1, 2014)

Abstract: An electrochemical biosensing platform was developed based on glucose oxidase (GOx)/Fe_3O_4-reduced graphene oxide (Fe_3O_4-RGO) nanosheets loaded on the magnetic glassy carbon electrode (MGCE). With the advantages of the magnetism, conductivity and biocompatibility of the Fe_3O_4-RGO nanosheets, the nanocomposites could be facilely adhered to the electrode surface by magnetically controllable assembling and beneficial to achieve the direct redox reactions and electrocatalytic behaviors of GOx immobilized into the nanocomposites. The biosensor exhibited good electrocatalytic activity, high sensitivity and stability. The current response is linear over glucose concentration ranging from 0.05 to 1.5 mM with a low detection limit of 0.15 μM. Meanwhile, validation of the applicability of the biosensor was carried out by determining glucose in serum samples. The proposed protocol is simple, inexpensive and convenient, which shows great potential in biosensing application.

Keywords: Fe_3O_4-reduced graphene oxide (Fe_3O_4-RGO); Nanocomposites; Magnetically controllable assembling; Direct electron transfer; Biosensor

Citation: Lili Yu, Hui Wu, Beina Wu, Ziyi Wang, Hongmei Cao, Congying Fu and Nengqin Jia, "Magnetic Fe_3O_4-Reduced Graphene Oxide Nanocomposites-Based Electrochemical Biosensing", Nano-Micro Lett. 6(3), 258-267 (2014). http://dx.doi.org/10.5101/nml140028a

Introduction

Diabetes mellitus is a worldwide public health problem, which resulted from either a deficiency or tolerance in insulin [1]. Glucose biosensors are becoming an indispensable means for the diagnosis and therapy of diabetes mellitus [2]. Amperometric enzyme electrodes based on glucose oxidase (GOx) have been extensively used for the detection of the blood glucose concentration due to the high catalytic activity for the oxidation of glucose to gluconolactone [3]. Nevertheless, the direct electron communication between redox proteins and electrode surfaces is difficult because the redox center in biomolecules is usually buried in the large three-dimensional structure of enzyme molecules [4,5]. Various materials have been studied to promote electron transfer of redox enzymes onto the surface of electrodes [6-9].

Magnetic nanomaterials have received much attention because of the unusual structural, excellent adsorption, catalytic properties and inherent electrical conductivity [10-14]. Graphene, a two-dimensional (2D) sheet of carbon atoms arranged in a honeycombed network, has perceived tremendous attention because of its high electrical conductivity, large surface area per volume, excellent electrocatalytic properties, all of which lead to their excellent performance as electrochemical biosensing platforms [15]. Furthermore, decoration with inorganic materials, such as metal or semiconductor nanoparticles (NPs) onto the reduced graphene oxide (RGO) sheets could form interesting 2D nanocomposite structures [16]. Fe_3O_4 magnetic NPs have been widely used in biomagnetics fields due to their magnetic properties, low toxicity, high adsorption ability and good biocompatibility [17-19]. Graphene sheets as

The Education Ministry Key Laboratory of Resource Chemistry and Shanghai Key Laboratory of Rare Earth Functional Materials, Department of Chemistry, College of Life and Environmental Sciences, Shanghai Normal University, Shanghai 200234, China
*Corresponding author: E-mail: nqjia@shnu.edu.cn

2D substrates can effectively prevent the agglomeration of Fe_3O_4 NPs and enable a good dispersion of these magnetic NPs [20]. In addition, Fe_3O_4-RGO nanocomposites may offer feasible biocompatible microenvironment, which preserves the biological and electrochemical activities of the immobilized biomolecules. Because of these fascinating properties, Fe_3O_4-RGO is promising as a potential magnetically controllable material for biosensor.

In this paper, magnetic Fe_3O_4-RGO nanosheets were prepared by a facile solvothermal method and characterized by transmission electron microscopy (TEM), atomic force microscopic (AFM) and X-ray diffraction spectra (XRD). Due to the inherent magnetic property and biocompatibility, the nanosheets could be served as a suitable substrate for the immobilization of GOx enzyme molecules and adhered to the magnetic electrode surface without any additional adhesive reagent. Thus the Fe_3O_4-RGO nanocomposites-based electrochemical biosensing systems were constructed by magnetically controllable assembling (Scheme 1). The direct electron transfer (DET) between the immobilized redox proteins and electrode was studied. Meanwhile, the developed biosensor showed good sensitivity, reproducibility and stability. The results indicated that magnetic Fe_3O_4-RGO based magnetically controllable protocol could reduce the analytes diffusion limitation, and well maintain the activity of enzyme. Therefore, this work provides a new avenue to broaden the applications of Fe_3O_4-RGO in electrochemical biosensors.

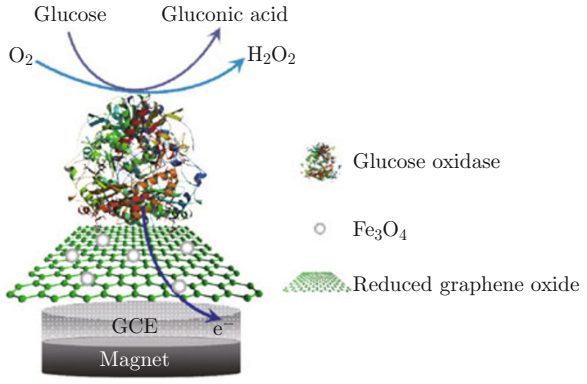

Scheme 1 Schematic illustration of Fe_3O_4-reduced graphene oxide nanocomposites-based electrochemical biosensors via magnetically controllable assembling.

Experimental

Reagents and materials

Graphite powder with 98% purity was purchased from Aladdin. Glucose oxidase (GOx, 100 U/mg) was purchased from Sangon Biotech. The D-(+)-Glucose was obtained from Sinopharm Chemical Reagent Co., Ltd. $FeCl_3{\cdot}6H_2O$, $FeCl_2{\cdot}4H_2O$, diethylene glycol (DEG), diethanolamine (DEA), sodium hydroxide, and ethanol were purchased from Sinopharm Chemical Reagent Co., Ltd. Glucose stock solutions (0.1 M) were prepared and allowed to mutarotate overnight at room temperature before use. Phosphate buffer solution (PBS, 0.1 M) was prepared from 0.1 M NaH_2PO_4 and Na_2HPO_4 in doubly distilled water and the pH was adjusted to 6.0. All other reagents used were of analytical grade, and all aqueous solutions were prepared with doubly distilled water.

Apparatus and measurements

JEOL 2100 transition electronic microscopy was used for transmission electron microscopy (TEM) analysis. Atomic force microscope (AFM) measurement was carried out on a MultiMode Nanoscope from digital instruments (Bruker AXS GmbH). X-ray diffraction patterns were collected on a Bragg-Brentano diffractometer (Rigaku D/Max-2000) with monochromatic Cu Kα radiation ($\lambda = 1.5418$ Å) of a graphite curve monochromator. UV-vis absorption spectra were recorded by a Multiskan spectrum with wavelength range of 200-1000 nm. Magnetic property was carried out at room temperature using a vibrating sample magnetometer (Lake Shore, VSM736).

All electrochemical measurements were performed on a CHI660B electrochemical workstation (Chenhua Instruments, Shanghai, China). Electrochemical experiments were performed with a conventional three-electrode system comprising of a bare or Fe_3O_4-RGO-modi?ed MGCE as the working electrode, a platinum wire as the counter electrode, and a saturated calomel electrode (SCE) as the reference electrode.

Synthesis of Fe_3O_4-RGO nanocomposites

Graphite oxide (GO) was prepared from natural graphite by the modified Hummer's method [21,22]. The superparamagnetic Fe_3O_4-RGO nanosheets were prepared via solvothermal method with some modification of those reported literatures [23,24]. In brief, a solution of $FeCl_2{\cdot}4H_2O$ (5 mmol) was mixed with $FeCl_36H_2O$ solution (10 mmol) and dissolved in 10 mL of hot DEG at 90℃ in an oil bath. After 30 min of stirring, 2.5 mL of DEA was added to the above solution. Meanwhile, NaOH (10 mmol) and DEG (20 mL) were mixed to produce a stock solution. The resulting solution was dropped into the hot iron solution under vigorous stirring for another 10 min. Subsequently, the homogeneous GO (15 mg) dispersion was mixed with DEG solution (10 mL) followed by 30 min of vigorous stirring. The mixture was then transferred to a Teflon-lined autoclave and maintained at 180℃ for 8 h. After centrifugation, the products were washed with ethanol and distilled water in turn until neutralization and dried under vacuum at room temperature finally.

Fabrication of GOx/Fe_3O_4-RGO/MGCE

The magnetic glassy carbon electrode (MGCE) was first polished to a mirror with 0.3 and 0.05 μm alumina slurry, and sonicated in ethanol and water successively. The electrodes were successively sonicated in 1:1 (v/v) nitric acid, acetone and ethanol, and then allowed to dry under a stream of nitrogen. For the preparation of GOx/Fe_3O_4-RGO modified electrode, MGCE was immersed in 0.2 mL as-prepared Fe_3O_4-RGO suspension (2 mg mL^{-1}) at room temperature. Fe_3O_4-RGO sheets were firmly attached to the electrode surface by a simple magnetically controllable absorption. After washing with water, the obtained Fe_3O_4-RGO/MGCE was dipped into GOx solution (3 mg mL^{-1} at pH 6.0) at 4℃ overnight for protein immobilization. The resulting electrodes were washed with water and stored at 4℃ when not in use.

Results and discussion

Characterization of Fe_3O_4-RGO nanocomposites

Transmission electron microscopy (TEM) was employed to characterize the dispersity and particle size of the prepared samples. Figure 1(a) presents representative TEM image of graphene nanosheets, clearly illustrating the flake-like shapes and a crumpled structure. These monolayer sheets possess large surface areas, and particles can be anchored on both sides of these sheets [20]. As shown in Fig. 1(b), Fe_3O_4 MNPs have been located on the RGO nanosheets. Furthermore, the anchored Fe_3O_4 metal NPs distributed uniformly on these graphene sheets without obvious aggregations.

Atomic force microscopic (AFM) images were recorded with a Nanoscope IIIa scanning probe microscope using a tapping mode. The sample used for AFM measurements was prepared by casting the suspension of GO or Fe_3O_4-RGO on the surface of a mica sheet and allowed to be evaporated. Typical AFM images of GO and Fe_3O_4-RGO nanosheets are presented in Fig. 2. The cross-sectional analysis indicates the mean thickness of GO (Fig. 2(a)) monolayer is ca. 1.0 nm, which is corresponding to previous report [25]. And the thickness of Fe_3O_4-RGO sheets (Fig. 2(b)) was determined to be ca. 18.0 nm, indicating the successful loading of Fe_3O_4 nanoparticles on the nanosheets.

The interconnected two-dimensional (2D) substrates could be served as a platform for enzyme immobilization through non-covalent adsorption and covalent binding [26]. Zeta potential measurements showed that after the surface modification with Fe_3O_4 nanoparticles, the Zeta potential value of GO dramatically changed from −43.7 mV to +31.5 mV. It may be due to the adsorption and complexing of DEA, thereby the surfaces of the as-prepared Fe_3O_4 nanoparticles are terminated with many NH_2 groups, which provide the surface of the magnetic nanosheets with positive charges [23] and benefit for further bioconjugates. Thus GOx molecules could easily be adsorbed on the Fe_3O_4-RGO, which are mainly dominated by the electrostatic interaction between positively charged Fe_3O_4-RGO nanocomposites and negatively charged enzyme molecules. In addition, other kinds of interaction such as hydrophobic attraction and hydrogen bonding might also be functioned in the adsorption process [27].

Representative X-ray diffraction (XRD) patterns of the prepared samples are depicted in Fig. 3(A). As shown in curve a, the characteristic diffraction peaks at 18° (111), 30° (220), 36° (311), 43° (400), 54° (422) and 57° (511) are consistent with the standard XRD data for the crystalline planes of face-centered cubic (fcc) Fe_3O_4 according to the standard spectrum of Fe_3O_4 (JCPDS, No. 65-3107). Besides these peaks, an additional peak at 26.0° corresponding to the RGO can be observed in curve b [28]. This indicated the coexistence of Fe_3O_4 and RGO in the hybrid. As shown in Fig. 3(B), the magnetic hysteresis loop of the Fe_3O_4-RGO hybrid is measured at room temperature with an applied magnetic field sweeping from −5000 to +5000 Oe, exhibiting superparamagnetic property of the magnetic nanocomposite [29].

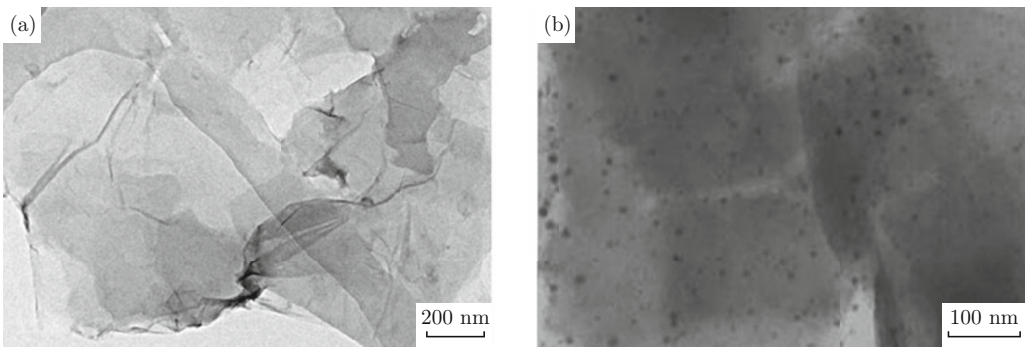

Fig. 1 TEM images of (a) GO and (b) Fe_3O_4-RGO nanosheets.

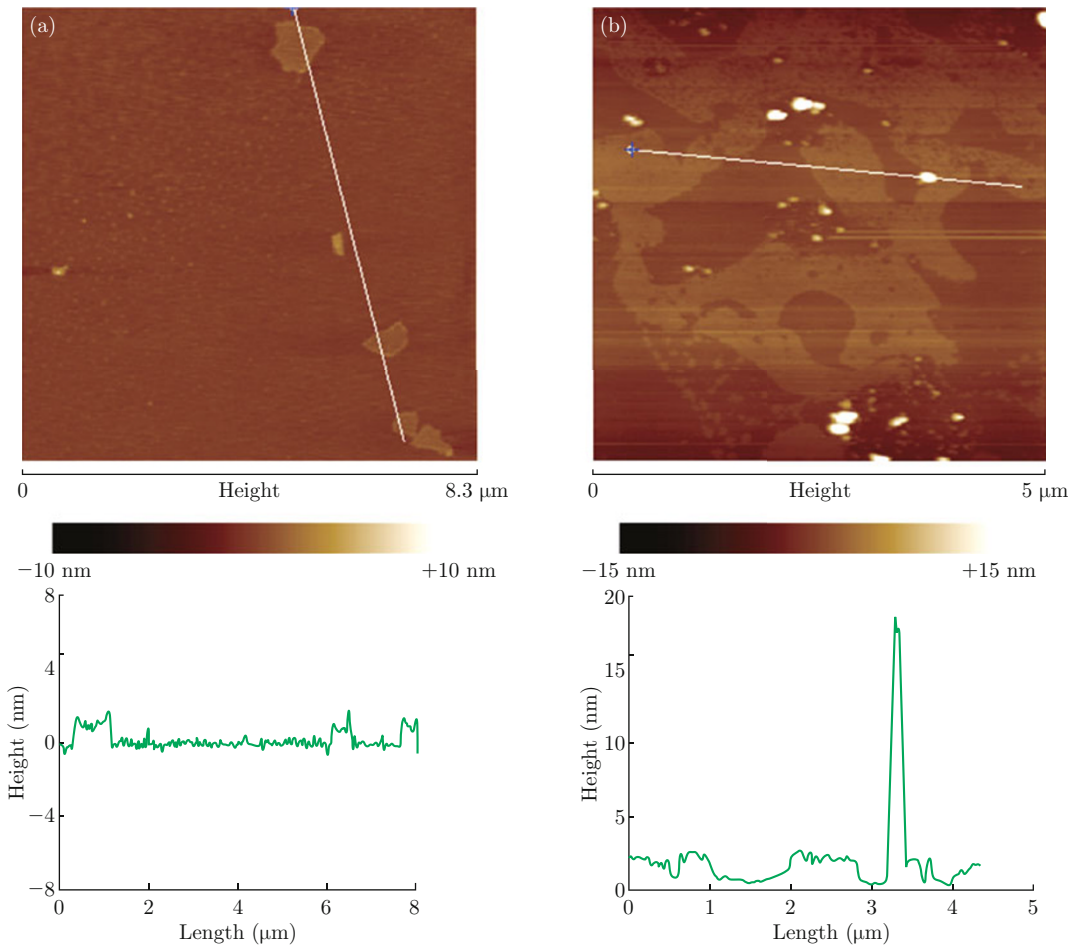

Fig. 2 AFM images of (a) GO and (b) Fe_3O_4-RGO nanosheets casting on freshly cleaved mica.

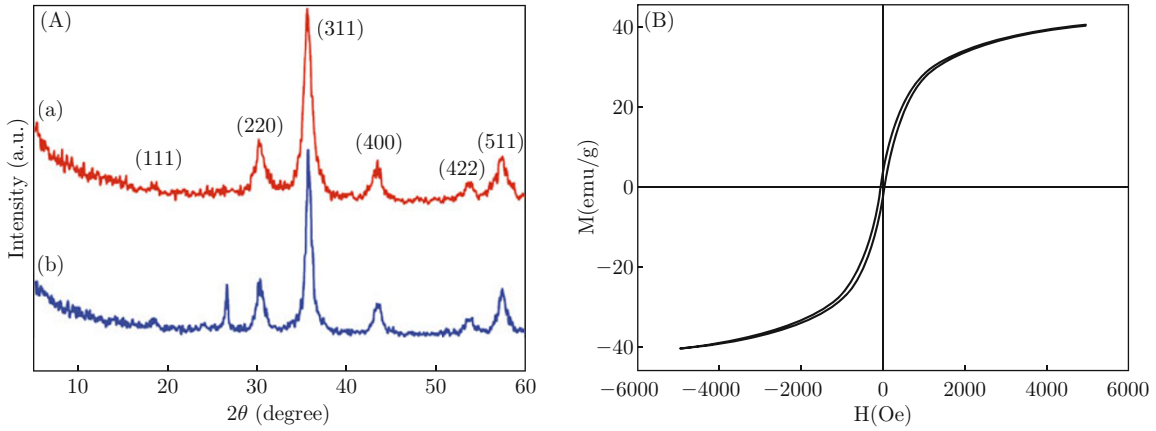

Fig. 3 (A) X-ray diffraction patterns of (a) Fe_3O_4; and (b) Fe_3O_4-RGO nanosheets. (B) Magnetization hysteresis loopof Fe_3O_4-RGO nanosheets.

UV-vis absorption spectra have been carried out to study the effects of Fe_3O_4-RGO on the microstructures of immobilized GOx. Figure 4(A) shows UV-vis absorption spectra of Fe_3O_4-RGO, GOx and the mixture of GOx and Fe_3O_4-RGO, respectively. As shown in Fig. 4(A), in the case of pure GOx an intense band appeared at 275 nm and two well defined peaks of light absorption at 375 nm and 452 nm (Fig. 4(A), curve a) could be distinguished [30]. The UV-vis spectra of the Fe_3O_4-RGO indicate no absorption peak appearing in the range of 250-500 nm (Fig. 4(A), curve b). After bioconjugation of GOx with Fe_3O_4-RGO (Fig. 4(A), curve c), there is nearly no change in the absorption band, similar to that of native GOx. The results indicated

that GOx entrapped in the nanocomposites has an unchanged secondary structure and retains its biological activity.

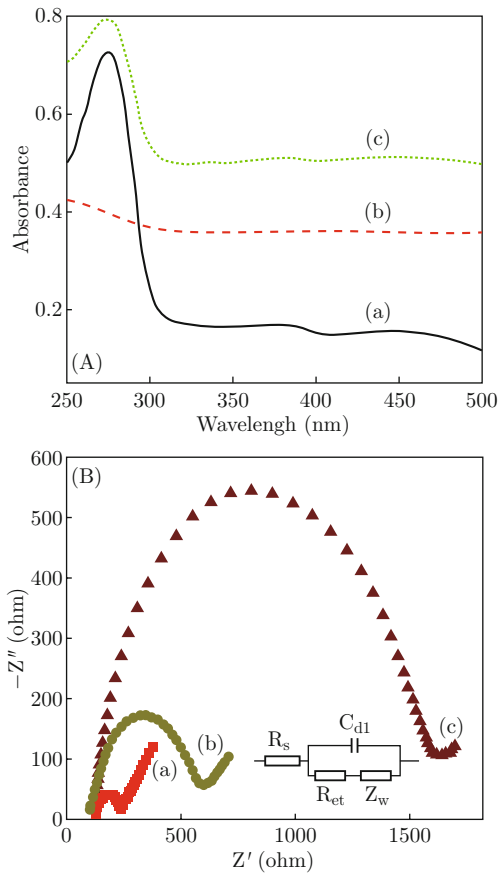

Fig. 4 (A) UV-vis absorbent spectra of (a) pure GOx; (b) Fe_3O_4-RGO and (c) GOx/RGO/Fe_3O_4. (B) Nyquist plots of faradic impedance obtained in 0.10 M PBS (pH 6.0) containing 1.0 mM $K_3Fe(CN)_6/K_4Fe(CN)_6$ and 0.1 M KCl for (a) bare MGCE; (b) Fe_3O_4-RGO modified MGCE; (c) Fe_3O_4-RGO-GOx modified MGCE. AC amplitude: 5 mV; frequency range: 0.1 Hz to 100 kHz. Inset: equivalent circuit used to model impedance data.

Electrochemical impedance spectroscopy (EIS) is a highly effective tool to measure the change of interface properties of the modified electrode surface during the fabrication process [31]. Figure 4(B) illustrates the typical Nyquist plots of the bare MGCE, Fe_3O_4-RGO/MGCE and GOx/Fe_3O_4-RGO/MGCE in the presence of 1.0 mM $K_3[Fe(CN)_6]/K_4[Fe(CN)_6]$. The EIS spectra shows well-defined semicircles at high frequencies followed by straight lines at low frequencies. The electron transfer resistance (R_{et}), estimated from the diameter of the semicircle, controls the electron transfer kinetics of the redox probe at the electrode interface. In order to give detailed information about the electrical properties of the above modified electrodes, the equivalent circuit (inset of Fig. 4(B)) was used to fit the obtained impedance data. As shown in Fig. 4(B), the R_{et} value of bare MGCE is estimated to be 160 Ω (Fig. 4(B), curve a). After MGCE modified with magnetic Fe_3O_4-RGO, the R_{et} value for the $[Fe(CN)_6]^{3-/4-}$ redox couple is increased (Fig. 4(B), curve b), which may be attributed that the amino groups and carboxyl functional groups on the surface of the nanosheets could block electron transmission to some extent. Comparison to the Fe_3O_4-RGO/MGCE, the EIS of the GOx/Fe_3O_4-RGO/MGCE presents an obvious increase in R_{et} (R_{et} = 513 Ω, Fig. 4(B), curve c). This increase is due to the non-conductive properties of GOx film, which hinders the interfacial electron transfer. It suggests that GOx molecules were successfully immobilized onto the Fe_3O_4-RGO nanocomposites modified electrode.

Direct electrochemistry of GOx/Fe_3O_4-RGO/MGCE

Figure 5(A) exhibits the cyclic voltammograms (CVs)

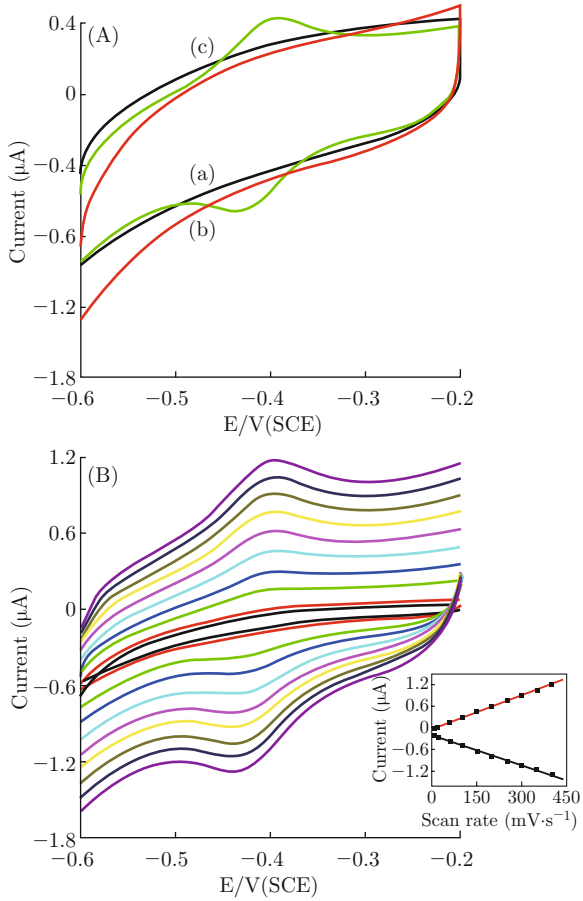

Fig. 5 (A) The CVs of different electrodes MGCE (a); Fe_3O_4-RGO/MGCE (b) and GOx/Fe_3O_4-RGO/MGCE (c)) in nitrogen-saturated 0.1 M PBS (pH 6.0) at the scan rate of 100 mV/s. (B) Cyclic voltammograms of GOx/Fe_3O_4-RGO/MGCE in 0.1 M nitrogen- saturated PBS (pH 6.0) at various scan rates (from inner to outer): 20, 10, 20, 40, 80, 100, and 400 mV s^{-1}. Inset: plots of peak currents (ip) vs. scan rates.

of the MGCE, Fe_3O_4-RGO/MGCE and GOx/ Fe_3O_4-RGO/MGCE in 0.1 M nitrogen-saturated PBS (pH 6.0) at a scan rate of 100 mV/s. It is found that there are no any redox peaks at the MGCE (Fig. 5(A), curve a) and Fe_3O_4-RGO/MGCE (Fig. 5(A), curve b), which indicates that Fe_3O_4-RGO is not electroactive in the potential range from −0.6 V to −0.2 V. Conversely, a pair of well-defined and nearly reversible redox waves could be observed at RGO/Fe_3O_4-GOx/MGCE. Its formal potential E^0 (defined as the average of the anodic and cathodic peak potential) is calculated to be −0.44 V, which is close to those previously reported for immobilized GOx [32,33]. This observation confirms the facile direct electron transfer from the redox site of GOx (flavin adenine dinucleotide) to the electrode. This result suggests that Fe_3O_4-RGO nanocomposites could provide a favorable microenvironment to facilitate the electron exchange between GOx and underlying electrode.

The effect of scan rates on the response of immobilized GOx is shown in Fig. 5(B). The anodic peak potential shifted to a more positive direction and the cathodic peak potential moved negatively with the increasing scan rate. However, formal potential of FAD/$FADH_2$ redox couple is nearly not changed. The linear dependence of I_{pa} and I_{pc} on scan rate is given in the inset of Fig. 5(B). The redox peak currents are directly proportional to the scan rate in the range of 10-400 mV s^{-1}, indicating a typical surface-controlled electrode process. According to the model of Laviron [34], the electron transfer rate constant (k_s) value is estimated to be 3.4 s^{-1}. This value is larger than those obtained for GOx immobilized on PMB@SiO_2(nano)/GCE (2.44 s^{-1}) [35] and GOx/BCNTs/MGCE (1.56 s^{-1}) [33], suggesting that the Fe_3O_4-RGO nanocomposites can greatly promote the electron exchange between active site of GOx and the electrode.

The pH-dependent response of the Fe_3O_4-RGO/GOx nanocomposite modified MGCE was also evaluated. As shown in Fig. 6(A), stable and well-defined reversible redox peaks are observed in the various pH solutions. Elevation of the solution pH from 4.5 to 8.0 leads to negative shift in both reduction and oxidation peak potentials. The slope of formal potential is estimated to be −58.4 mV/pH (Fig. 6(B)), which is close to the theoretical value of −58.5 mV/pH [36]. The results indicate that two-proton coupled with two-electron accompanies the electron transfer of GOx (FAD) to electrodes.

Electrocatalytical behavior of the Fe_3O_4-RGO-GOx/MGCE

Figure 7(A) shows cyclic voltammograms of GOx/ Fe_3O_4-RGO/MGCE in N_2-saturated solution (Fig. 7(A), curve a), air-saturated solution without

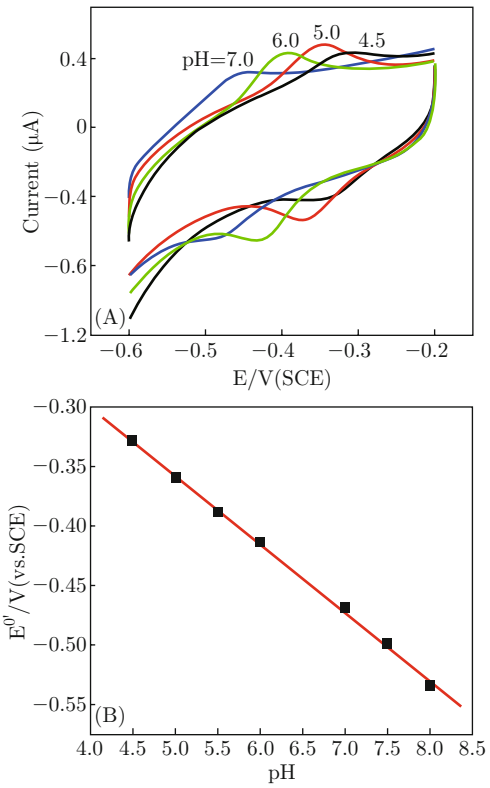

Fig. 6 (A) Cyclic voltammograms of the GOx/Fe_3O_4-RGO/MGCE in 0.1 M deoxygenated solution with different pH values (7.0, 6.0, 5.0 and 4.5), scan rate: 100 mV s^{-1}. (B) Plot of formal potential (E^0) vs. pH values.

(Fig. 7(A), curve b) and with (Fig. 7(A), curve c) 1.0 mM glucose. A pair of redox peaks is observed in both N_2-saturated and air-saturated 0.1 M PBS (pH 6.0) solution. Under N_2-saturated condition, there appears a pair of well-defined and reversible redox peaks (Fig. 7(A), curve a). However, in the presence of dissolved oxygen (Fig. 7(A), curve b), original oxidation peak decreases and reduction peak increases. The results indicate that GOx immobilized on Fe_3O_4-RGO/MGCE can catalyze the reduction of dissolved oxygen. This electrocatalytic process toward the reduction of dissolved oxygen may be expressed as follows: [6,35,37]

$$\mathrm{GOx(FAD)} + 2e^- + 2H^+ \rightleftharpoons \mathrm{GOx(FADH_2)} \quad (1)$$

$$\mathrm{GOx(FADH_2)} + O_2 \rightarrow \mathrm{GOx(FAD)} + H_2O_2 \quad (2)$$

When glucose was added into air-saturated PBS, the reduction peak current at the GOx/Fe_3O_4-RGO/MGCE decreased (Fig. 7(A), curve c). It can be explained that glucose as the substrate of GOx can result in an enzyme-catalyzed reaction (Eq. (3)) and decrease the amount of the oxidized form (FAD) of GOx on the electrode surface.

$$\mathrm{Glucose} + \mathrm{GOx(FAD)} \rightarrow \mathrm{gluconolactone} + \mathrm{GOx(FADH_2)} \quad (3)$$

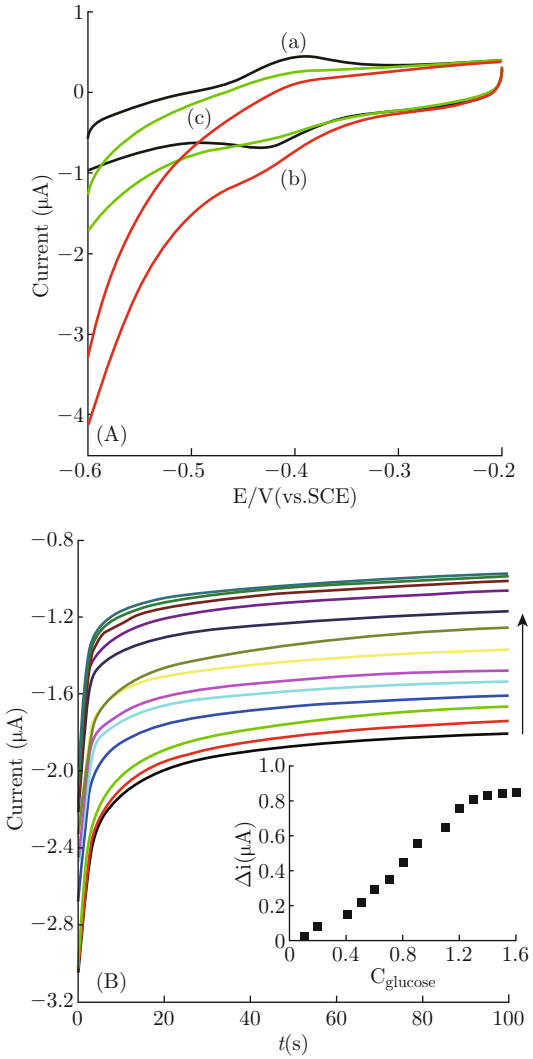

Fig. 7 (A) Cyclic voltammograms of the GOx/Fe_3O_4-RGO/MGCE in 0.1 M deoxygenated (a) and air-saturated PBS (pH 6.0) without (b) and with 1 mM glucose (c) at the scan rate of 100 mV s^{-1}. (B) Amperometric curves of GOx/Fe_3O_4-RGO modified electrode in 0.1 M pH 6.0 air-saturated PBS with the addition of a series of glucose concentrations. Inset: calibration curve corresponding to amperometric responses. Applied potential: −0.5V (vs. SCE).

Thus, the addition of glucose restrains the electrocatalytic reaction (Eq. (1)), and leads to the decrease of reduction current. Therefore, in this way, based on measuring the decrease of the reduction current at the relatively negative potential, the concentration of glucose can be detected without the interference of coexisted electroactive-substance.

The amperometric responses of GOx/Fe_3O_4-RGO/MGCE in air-saturated 0.1 M PBS (pH 6.0) with different glucose concentration are shown in Fig. 7(B). Chronoamperometric curves are found to reach a plateau (steady-state current) within 20 s. With the successive addition of glucose, the amperometric responses decrease, indicating the electrochemical signal is dependent on the concentration of glucose. Therefore, the results of amperometric responses are in correspondence with those of the above CV measurements. The developed biosensor shows a steady state amperometric response towards glucose in the range of 0.05-1.5 mM with a detection limit of 0.15 μM (S/N = 3 and inset in Fig. 7(B)). The sensitivity of the enzyme electrode was calculated to be about 9.04 μA mM^{-1} cm^{-2}, which was higher than those reported at a GOx/TiO_2-SWCNT/ITO-based glucose biosensor (5.32 μA mM^{-1} cm^{-2}) [38] and GOx/titania sol/gel film (7.2μA mM^{-1} cm^{-2}) [39]. Furthermore, according to the electrochemical version of the Lineweaver-Burk plot [40], the apparent Michaelis-Menten constant (K_m^{app}) for the GOx/Fe_3O_4-RGO/MGCE is estimated to be 0.34 mM, which is smaller than that of GOx on nitrogen-doped carbon nanotubes of 2.2 mM [41]. The smaller K_m^{app} value indicates that the immobilized GOx possesses high enzymatic activity and the biosensor exhibits a high affinity for glucose.

Furthermore, the stability and real sample analysis of the biosensor were investigated. The GOx-Fe_3O_4-RGO/MGCE could retain the direct electrochemistry of the immobilized GOx at constant current values upon the continuous cyclic voltammograms sweep over several hundred cycles. No obvious decrease in the current response to glucose was observed after one month storage in the refrigerator at 4℃. Human serum samples were assayed to testify the practical use of the proposed biosensor. The recovery experiments were carried out in diluted human serum samples, using a standard addition method. As presented in Table 1, the recovery of the biosensor is between 95% and 105%. The results indicate that the biosensor is effective and sensitive for the determination of glucose in real samples.

Table 1 Determination of glucose concentration in human serum samples using the GOx-Fe_3O_4/reduced graphene oxide/MGCE

Sample	Added (nM)	Found (mM)	Recovery (%)
1	0.15	0.17	96.66
2	0.80	0.82	102.50
3	1.00	0.98	98.07

Conclusions

To summarize, we constructed a magnetic Fe_3O_4-reduced graphene oxide nanocomposites-based on electrochemical biosensing system for glucose determination. Owing to their excellent magnetic property and biocompatibility, Fe_3O_4-RGO nanocomposites could be used as suitable matrix for the immobilization of GOx enzyme and conveniently loaded on the surface of magnetic glass carbon electrodes by magnetically con-

trollable assembling. The direct electron transfer of GOx assembled on Fe_3O_4-RGO nanosheets could be achieved, indicating that nanocomposites provide a favorable microenvironment to facilitate the electron exchange between enzyme and electrode. The developed biosensor exhibited good electrocatalytic activity toward glucose, and could be effectively applied for glucose measurements in real samples.

Acknowledgements

This work was supported by the National Natural Science Foundation of China (21373138), Shanghai Sci. & Tech. Committee (12JC1407200), Program for Changjiang Scholars and Innovative Research Team in University (IRT1269).

References

[1] S. P. Nichols, A. Koh, W. L. Storm, J. H. Shin and M. H. Schoenfisch, "Biocompatible materials for continuous glucose monitoring devices", Chem. Soc. Rev. 113(4), 2528-2549 (2013). http://dx.doi.org/10.1021/cr300387j

[2] C. Qiu, X. Wang, X. Liu, S. Hou and H. Ma, "Direct electrochemistry of glucose oxidase immobilized on nanostructured gold thin films and its application to bioelectrochemical glucose sensor", Electrochim. Acta 67, 140-146 (2012). http://dx.doi.org/10.1016/j.electacta.2012.02.011

[3] C. He, J. Liu, Q. Zhang and C. Wu, "A novel stable amperometric glucose biosensor based on the adsorption of glucose oxidase on poly(methyl methacrylate)-bovine serum albumin core-shell nanoparticles", Sensor. Actuat. B: Chem. 166-167, 802-808 (2012). http://dx.doi.org/10.1016/j.snb.2012.03.081

[4] C. Fu, W. Yang, X. Chen and D. G. Evans, "Direct electrochemistry of glucose oxidase on a graphite nanosheet-Nafion composite film modified electrode", Electrochem. Commun. 11(5), 997-1000 (2009). http://dx.doi.org/10.1016/j.elecom.2009.02.042

[5] X. Kang, J. Wang, H. Wu, I. A. Aksay, J. Liu and Y. Lin, "Glucose oxidase-graphene-chitosan modified electrode for direct electrochemistry and glucose sensing", Biosens. Bioelectron. 25(4), 901-905 (2009). http://dx.doi.org/10.1016/j.bios.2009.09.004

[6] S. Liu and H. Ju, "Reagentless glucose biosensor based on direct electron transfer of glucose oxidase immobilized on colloidal gold modified carbon paste electrode", Biosens. Bioelectron. 19(3), 177-183 (2003). http://dx.doi.org/10.1016/S0956-5663(03)00172-6

[7] Y. Song, K. Qu, C. Zhao, J. Ren and X. Qu, "Graphene oxide: intrinsic peroxidase catalytic activity and its application to glucose detection", Adv. Mater. 22(19), 2206-2210 (2010). http://dx.doi.org/10.1002/adma.200903783

[8] S. Su, Y. He, S. Song, D. Li, L. Wang, C. Fan and S. T. Lee, "A silicon nanowire-based electrochemical glucose biosensor with high electrocatalytic activity and sensitivity", Nanoscale 2(9), 1704-1707 (2010). http://dx.doi.org/10.1039/C0NR00314J

[9] S. A. Ansari and Q. Husain, "Potential applications of enzymes immobilized on/in nano materials: a review", Biotechnol. Adv. 30(3), 512-523 (2012). http://dx.doi.org/10.1016/j.biotechadv.2011.09.005

[10] J. D. Qiu, H. P. Peng R. P. Liang and X. H. Xia, "Facile preparation of magnetic core-shell Fe_3O_4@Au nanoparticle/myoglobin biofilm for direct electrochemistry", Biosens. Bioelectron. 25(6), 1447-1453 (2010). http://dx.doi.org/10.1016/j.bios.2009.10.043

[11] H. P. Peng, R. P. Liang and J. D. Qiu, "Facile synthesis of Fe_3O_4@Al_2O_3 core-shell nanoparticles and their application to the highly specific capture of heme proteins for direct electrochemistry", Biosens. Bioelectron. 26(6), 3005-3011 (2011). http://dx.doi.org/10.1016/j.bios.2010.12.003

[12] H. P. Peng, R. P. Liang, L. Zhang and J. D. Qiu, "Sonochemical synthesis of magnetic core-shell Fe_3O_4@ZrO_2 nanoparticles and their application to the highly effective immobilization of myoglobin for direct electrochemistry", Electrochim. Acta 56(11), 4231-4236 (2011). http://dx.doi.org/10.1016/j.electacta.2011.01.090

[13] C. Zou, Y. Fu, Q. Xie and S. Yao, "High-performance glucose amperometric biosensor based on magnetic polymeric bionanocomposites", Biosens. Bioelectron. 25(6), 1277-1282 (2010). http://dx.doi.org/10.1016/j.bios.2009.10.014

[14] S. Wu, H. Wang, S. Tao, C. Wang, L. Zhang, Z. Liu and C. Meng, "Magnetic loading of tyrosinase-Fe_3O_4/mesoporous silica core/shell microspheres for high sensitive electrochemical biosensing", Anal. Chem. Acta 686(1-2), 81-86 (2011). http://dx.doi.org/10.1016/j.aca.2010.11.053

[15] D. Chen H. Feng and J. Li, "Graphene oxide: preparation, functionalization, and electrochemical applications", Chem. Rev. 112(11), 6027-6053 (2012). http://dx.doi.org/10.1021/cr300115g

[16] I. V. Lightcap T. H. Kosel and P. V. Kamat, "Anchoring semiconductor and metal nanoparticles on a two-dimensional catalyst mat. storing and shuttling electrons with reduced graphene oxide", Nano Lett. 10(2), 577-583 (2010). http://dx.doi.org/10.1021/nl9035109

[17] Q. Chang, K. Deng, L. Zhu, G. Jiang, C. Yu and H. Tang, "Determination of hydrogen peroxide with the aid of peroxidase-like Fe_3O_4 magnetic nanoparticles as the catalyst", Microchim. Acta

165(3-4), 299-305 (2009). http://dx.doi.org/10.1007/s00604-008-0133-z

[18] Y. Cheng, Y. Liu, J. Huang, K. Li, Y. Xian, W. Zhang and L. Jin, "Amperometric tyrosinase biosensor based on Fe_3O_4 nanoparticles-coated carbon nanotubes nanocomposite for rapid detection of coliforms", Electrochim. Acta 54(9), 2588-2594 (2009). http://dx.doi.org/10.1016/j.electacta.2008.10.072

[19] G. Gao, H. Wu, Y. Zhang, K. Wang, P. Huang, X. Zhang, S. Guo and D. Cui, "One-step synthesis of Fe_3O_4@C nanotubes for the immobilization of adriamycin", J. Mater. Chem. 21(33), 12224-12227 (2011). http://dx.doi.org/10.1039/C1JM12535D

[20] W. Fan, W. Gao, C. Zhang, W. W. Tjiu, J. Pan and T. Liu, "Hybridization of graphene sheets and carbon-coated Fe_3O_4 nanoparticles as a synergistic adsorbent of organic dyes", J. Mater. Chem. 22(48), 25108-25115 (2012). http://dx.doi.org/10.1039/C2JM35609K

[21] J. Liang, Y. Xu, D. Sui, L. Zhang, Y. Huang, Y. Ma, F. Li and Y. Chen, "Flexible, magnetic, and electrically conductive graphene/Fe_3O_4 paper and its application for magnetic-controlled switches", J. Phys. Chem. C 114(41), 17465-17471 (2010). http://dx.doi.org/10.1021/jp105629r

[22] Y. Wang, H. Zhang, D. Yao, J. Pu, Y. Zhang, X. Gao and Y. Sun, "Direct electrochemistry of hemoglobin on graphene/Fe_3O_4 nanocomposite-modified glass carbon electrode and its sensitive detection for hydrogen peroxide", J. Solid. State. Electr. 17(3), 881-887 (2013). http://dx.doi.org/10.1007/s10008-012-1939-5

[23] M. Chen, Y. N. Kim, C. Li and S. O. Cho, "Preparation and characterization of magnetic nanoparticles and their silica egg-yolk-like nanostructures: a prospective multifunctional nanostructure platform", J. Phys. Chem. C 112(17), 6710-6716 (2008). http://dx.doi.org/10.1021/jp710775j

[24] H. Wu, G. Liu, Y. Zhuang, D. Wu, H. Zhang, H. Yang, H. Hu and S. Yang, "The behavior after intravenous injection in mice of multiwalled carbon nanotube/Fe_3O_4 hybrid MRI contrast agents", Biomaterials 32(21), 4867-4876 (2011). http://dx.doi.org/10.1016/j.biomaterials.2011.03.024

[25] D. P. Yang, X. Wang, X. Guo, X. Zhi, K. Wang, C. Li, G. Huang, G. Shen, Y. Mei and D. Cui, "UV/O_3 generated graphene nanomesh: formation mechanism, properties, and FET studies", J. Phys. Chem. C 118(1), 725-731 (2013). http://dx.doi.org/10.1021/jp409898d

[26] Y. Zhang, C. Wu, S. Guo and J. Zhang, "Interactions of graphene and graphene oxide with proteins and peptides", Nanotechnol. Rev. 2(1), 27-45 (2013). http://dx.doi.org/10.1515/ntrev-2012-0078

[27] G. Zhao, J. J. Feng, J. J. Xu and H. Y. Chen, "Direct electrochemistry and electrocatalysis of heme proteins immobilized on self-assembled ZrO_2 film", Electrochem. Commun. 7(7), 724-729 (2005). http://dx.doi.org/10.1016/j.elecom.2005.04.026

[28] I. K. Moon, J. Lee, R. S. Ruoff and H. Lee, "Reduced graphene oxide by chemical graphitization", Nat. Commun. 1, 73-78 (2010). http://dx.doi.org/10.1038/ncomms1067

[29] H. He and C. Gao, "Supraparamagnetic, conductive, and processable multifunctional graphene nanosheets coated with high-density Fe_3O_4 nanoparticles", ACS Appl. Mater. Interfaces 2(11), 3201-3210 (2010). http://dx.doi.org/10.1021/am100673g

[30] S. Z. Zhao, K. Zhang, Y. Bai, W. Yang and C. Sun, "Glucose oxidase/colloidal gold nanoparticles immobilized in Nafion film on glassy carbon electrode: direct electron transfer and electrocatalysis", Bioelectrochemistry 69(2), 158-163 (2006). http://dx.doi.org/10.1016/j.bioelechem.2006.01.001

[31] C. Hu, D. P. Yang, Z. Wang, L. Yu, J. Zhang and N. Jia, "Improved EIS performance of an electrochemical cytosensor using three-dimensional architecture Au@BSA as sensing layer", Anal. Chem. 85(10), 5200-5206 (2013). http://dx.doi.org/10.1021/ac400556q

[32] B. Unnikrishnan, S. Palanisamy and S. M. Chen, "A simple electrochemical approach to fabricate a glucose biosensor based on graphene-glucose oxidase biocomposite", Biosens. Bioelectron. 39(1), 70-75 (2013). http://dx.doi.org/10.1016/j.bios.2012.06.045

[33] C. Shan, H. Yang, J. Song, D. Han, A. Ivaska and L. Niu, "Direct electrochemistry of glucose oxidase and biosensing for glucose based on graphene", Anal. Chem. 81(6), 2378-2382 (2009). http://dx.doi.org/10.1021/ac802193c

[34] E. Laviron, "General expression of the linear potential sweep voltammogram in the case of diffusionless electrochemical systems", J. Electroanal. Chem. Interfacial Electrochem. 101(1), 19-28 (1979). http://dx.doi.org/10.1016/S0022-0728(79)80075-3

[35] X. Xiao, B. Zhou, L. Zhu, L. Xu, L. Tan, H. Tang, Y. Zhang, Q. Xie and S. Yao, "An reagentless glucose biosensor based on direct electrochemistry of glucose oxidase immobilized on poly(methylene blue) doped silica nanocomposites", Sensor. Actuat. B: Chem. 165(1), 126-132 (2012). http://dx.doi.org/10.1016/j.snb.2012.02.029

[36] K. Wang, H. Yang, L. Zhu, Z. Ma, S. Xing, Q. Lv, J. Liao, C. Liu and W. Xing, "Direct electron transfer and electrocatalysis of glucose oxidase immobilized on glassy carbon electrode modified with Nafion and mesoporous carbon FDU-15", Electrochim. Acta 54(20), 4626-4630 (2009). http://dx.doi.org/10.1016/j.electacta.2009.02.097

[37] P. Wu, Q. Shao, Y. Hu, J. Jin, Y. Yin, H. Zhang and C. Cai, "Direct electrochemistry of glucose oxidase assembled on graphene and application to glucose detection", Electrochim. Acta

55(28), 8606-8614 (2010). http://dx.doi.org/10.1016/j.electacta.2010.07.079

[38] N. Q. Dung, D. Patil, T. T. Duong, H. Jung, D. Kim and S. G. Yoon, "An amperometric glucose biosensor based on a GOx-entrapped TiO_2-SWCNT composite", Sensor. Actuat. B: Chem. 166-167(0), 103-109 (2012). http://dx.doi.org/10.1016/j.snb.2012.01.008

[39] J. Yu, S. Liu and H. Ju, "Glucose sensor for flow injection analysis of serum glucose based on immobilization of glucose oxidase in titania sol-gel membrane", Biosens. Bioelectron. 19(4), 401-409 (2003). http://dx.doi.org/10.1016/S0956-5663(03)00199-4

[40] D. L. Scott and E. F. Bowden, "Enzyme-substrate kinetics of adsorbed cytochrome c peroxidase on pyrolytic graphite electrodes", Anal. Chem. 66(8), 1217-1223 (1994). http://dx.doi.org/10.1021/ac00080a004

[41] S. Deng, G. Jian, J. Lei, Z. Hu and H. Ju, "A glucose biosensor based on direct electrochemistry of glucose oxidase immobilized on nitrogen-doped carbon nanotubes", Biosens. Bioelectron. 25(2), 373-377 (2009). http://dx.doi.org/10.1016/j.bios.2009.07.016